Investigating the impact of weather variables on the energy yield and cost of energy of grid-connected solar concentrator systems

Eduardo F. Fernández[1,2*], Diego L. Talavera[2], Florencia M. Almonacid[1,2] and Greg P. Smestad[3]

[1]*Centre for Advanced Studies in Energy and Environment, University of Jaen, Las Lagunillas Campus, Jaen 23071, Spain*

[2]*IDEA Solar Energy Research Group, University of Jaen, Las Lagunillas Campus, Jaen 23071, Spain*

[3]*Sol Ideas Technology Development, San José, California 95150-5729, USA*

[*]*Corresponding author: fenandez@ujaen.es, +34 9543213520*

Abstract

This work connects the electrical performance and economics of High Concentrator Photovoltaic technology beyond the cell and module levels. It analyses the impact of fundamental variables on the calculated energy output and economics of a typical system for real-world solar power plants in five locations with diverse climatic conditions. It was found that there exists a nearly linear relationship between the Final Energy Yield and the average direct normal irradiance, while the cell temperature and spectral AC energy losses ranged from 4.6 % to 1.8 % and 5.0 % to 2.4 %. The Levelised Cost of Electricity (LCOE) calculations used these insights, together with the specific economic values for each location. The results show that the locations with the higher annual energy yield tend to have the lower LCOE values. In particular, the LCOE ranged from 5.5 c€/kWh to 22.2 c€/kWh for a conservative scenario. However, the sites with the highest final yield do not necessarily present the lowest values of LCOE. The results emphasize the interrelationship between the instantaneous effects of cell temperature and spectrum on the performance of the system, as well as the importance of considering the specific economic parameters to estimate the LCOE at each location.

Keywords: energy yield, energy economics, Levelised Cost of Electricity (LCOE), high concentrator photovoltaics (HCPV), solar resource, atmospheric variables.

Nomenclature

Symbol	Definition	Units
A_{module}	Area of the modules	m^2
b_0, b_1 and b_2	Coefficients for the inverter	dimensionless
d	Nominal discount rate	%
DEP_y	Annual tax depreciation	€/kWp
DNI	Direct Normal Irradiance	W/m^2
DNI_{heat}	Portion of the direct normal irradiance transformed into heat	W/m^2
d_s	Annual dividend of the equity capital	%
E	Energy output	kWh

f	Instantaneous power correction function	W or dimensionless
$HCPV_{AOM}$	Annual operation and maintenance cost	€/kWp
$HCPV_I$	Initial investment cost	€/kWp
$HCPV_l$	Amount equal to the portion of the initial investment financed with the loan	%
$HCPV_s$	Amount equal to the portion of the initial investment financed with equity	%
i	Annual inflation rate	%
i_l	Annual loan interest rate	%
L	Power conversion losses	dimensionless
LCC	Life cycle cost of the system	€/kWp
LCOE	Levelised Cost of Electricity	€/kWh
N	Life cycle (useful lifespan) of the system	years
N_d	Tax life for depreciation	years
N_l	Loan duration	years
N_S	Number of modules in series	dimensionless
N_P	Number of modules in parallel	dimensionless
P	Maximum power	W
p_{in}	Normalized inverter input power	dimensionless
PR	Performance Ratio of the system ($PR = Y_F/\Sigma DNI$)	%
PW [$DEP(N_d)$]	Present worth of the tax depreciation	€/kWp
PW[$HCPV_{OM}$ (N)]	Present worth of operation and maintenance cost	€/kWp
r_d	Annual degradation rate of the efficiency of the system	%
$r_{O\&M}$	Operation and maintenance cost of the system	€/kWp
R_{total}	Thermal resistance of the modules	$^oC/Wm^{-2}$
T	Income tax rate	%
T_{air}	Air temperature	^oC
T_C	Cell temperature	^oC
WACC	Weighted average cost of capital	%
Y_F	Final energy yield	kWh/kWp

Greek letters

δ	Temperature coefficient of maximum power	%/^{o}C
ε	Air mass coefficient of maximum power	%
φ	Aerosol optical depth coefficient of maximum power	%
$\eta_{inverter}$	Efficiency of the inverter	%

Subscripts and superscripts

*	Values at reference conditions
550	550 nm (AOD)
AC	AC electricity
DC	DC electricity
DNI	Direct Normal Irradiance
inverter	Inverter of the system
module	Module of the system

nominal	Nominal power (inverter)
o	Peak power (system)
S_b	Spectral direct normal irradiance
T_c	Cell temperature
U	Umbral value

Abbreviations

AERONET	Aerosol Robotic Network
AM	Air Mass
AOD	Aerosol Optical Depth
BOS	Balance of System
CDM	Clean Development Mechanism
CEAEMA	Centro de Estudios Avanzados en Energía y Medio Ambiente
CSTC	Concentrator Standard Test Conditions
EQE	External Quantum Efficiency
HCPV	High Concentrator Photovoltaics
MJ	Multi-junction (solar cell)
PMMA	Poly(methylmethacrylate) (Fresnel lens)
POE	Primary optical element
PV	Photovoltaics
SMARTS	Simple Model of the Atmospherics Radiative Transfer of Sunshine
SOE	Secondary optical element

1. Introduction

High Concentrator Photovoltaic (HCPV) technology represents a promising energy source to produce more cost-effective electricity compared to conventional Photovoltaic (PV) technology by reducing the amount of expensive semiconductor material used for the cell by using less expensive optical elements [1]. Currently, this technology is largely based on the use of high efficiency III-V concentrator multi-junction (MJ) solar cells consisting of several p-n junctions, usually three, to increase the absorption of the incident solar spectrum, and thus maximize the efficiency of the solar conversion device [2, 3]. The most widely used optical configuration consist of a primary optical element (POE), usually Fresnel lenses, and a secondary optical element (SOE). The aim of the POE is to collect and concentrate the direct rays, while the aim of the SOE is to receive the light from the POE to homogenize the luminous power on the solar cell surface and improve the acceptance angle of the overall concentrator system [4, 5]. An HCPV module is the fundamental unit of an HCPV system used to convert the direct sunlight into electricity. It consists of a particular number of MJ solar cells and concentrator optical units, and other peripheral components necessary to generate electricity and dissipate the heat produced by the high energy flux of concentrated sunlight [6]. Passive cooling mechanisms are mainly used because of their simplicity and reliability [7, 8, 9]. Finally, a typical grid-connected system consists of several modules interconnected in series and parallel mounted on a high precision pedestal. This two-axis solar tracker is connected to a high efficiency DC/AC inverter and the rest of balance of system components (BOS) [10, 11, 12]. The tracker allows for the optical axis

of the concentrator optics to be within < 1° of the solar disk. The efficiency of MJ concentrator cells, HCPV modules and systems is increasing over time, and is expected to reach values up to 50%, 45% and 40%, respectively, within the next few years [13, 14]. Moreover, the costs of electricity for this technology has shown decreasing trends and has already shown promising results at locations with high solar resource [15, 16]. The comments above show the great potential of this technology as an alternative renewable power source to play an important share in the global energy market [17].

Despite such excellent potential, different barriers must still be eliminated to increase the confidence of investors, and thus, to promote the market expansion of concentrator technology as a real alternative to traditional PV. Among all of them, the following two main concerns can be cited [18]: on the one hand, the understanding of the performance of HCPV systems when operating in real world conditions is clearly lower than conventional PV systems [19, 20]; on the other hand, the cost of electricity and bankability of HCPV technology needs to be more thoroughly studied [15, 21].

The electrical modelling of HCPV devices is inherently different and more complex than conventional PV devices. As in other types of PV technology, the energy output of HCPV is mainly determined by the irradiance, temperature and spectrum [19]. However, for instance, HCPV only collects the direct component of the irradiance due to the use of optical devices and the thermodynamic connections between concentration ratio and acceptance angle. Moreover, this aspect has demonstrated to be, by far, the most relevant variable to determine the performance of HCPV systems in the outdoors [20]. At the same time, the energy output of MJ solar cells is strongly affected by the spectral changes produced by the time-varying atmospheric parameters [22, 23], due to the series connection of several subcells with different energy gaps [24]. Therefore, the input spectrum also plays a crucial role in determining the energy output of HCPV modules or systems [25, 26]. The current-voltage characteristics of MJ solar cells are also affected by temperature [27, 28]. Under real-world working conditions, the operating cell temperature of HCPV systems is also affected by the weather variables [29]. So, the performance of HCPV modules or outdoor systems is also going to be determined by their cell operating temperature [30]. However, the measurement and/or estimation of the cell temperature is a complex task due to the fact that the MJ cells mounted on HCPV modules are surrounded by several peripheral elements [31]. During recent years, the HCPV community has devoted large efforts to develop tools tailored to the specific features of HCPV technology [32, 33], and has attempted to quantify the impact of the parameters described above on the performance of HCPV devices when operating in a deployed installation [19, 20, 22, 23, 26, 34, 35, 36]. Despite this, the majority of these studies are limited to the cell or module level, and there is a clear lack of studies concerning the analysis of the impact of the variables on the energy performance of complete HCPV systems found in solar power plants [21, 37, 38, 39].

At the same time, the cost of electricity is directly affected by the energy output of HPCV systems under real conditions. Hence, due to the lack of studies about this issue, and because HCPV is a relatively new technology, there is also an important lack of studies about the cost of electricity of this emerging technology [40, 41]. A report analysing the Levelised Cost of

Electricity (LCOE) of two systems at two locations with different irradiation levels in Germany was presented by the Fraunhofer ISE [42]. An analysis of the LCOE of two systems at two locations with different irradiation levels in USA was also presented by SolFocus Inc. [43]. A more complete analysis of the LCOE of a typical HCPV system covering all the irradiation levels of Spain has recently been presented by Talavera et al. [15].

The goal of this paper is to relate the calculated electrical performance of a representative HCPV system deployed at several locations to its corresponding LCOE. We analyse the performance and quantify the temperature and spectral losses in the AC energy output of a typical HCPV system at locations with disparate climate conditions. We then analyse the LCOE and quantify the temperature and spectral impacts on it using economic scenarios relevant to those locations. To our knowledge, these types of analyses have not previously been undertaken using this approach. For the estimation of the AC energy output, we use a typical HCPV system studied experimentally, together with a model previously introduced by Fernandez et al. [38]. For the analysis of the cost of electricity, we shall use the LCOE method, since it is the most widely used method to describe and compare both renewable and conventional energies, as considered in the literature [15, 16].

2. Concentrator system description

The HCPV system used in this study is located at the Centre for Advanced Studies in Energy and Environment (CEAEMA) of the University of Jaen in southern Spain (N 37º27´36´´, W 03º28´12´´). The HCPV modules of the generator are made up of 25 triple-junction lattice-matched GaInP/GaInAs/Ge solar cells interconnected in series, PMMA poly(methylmethacrylate) Fresnel lenses as a POE (primary optical element) and refractive truncated pyramids as the SOE (secondary optical elements). The modules have an optical efficiency of 85 %, a geometric concentration of 550x and use passive cooling based on an aluminium plate to maintain the temperature of concentrator solar cells within their optimal operating range (50-80 ^{o}C). Figure 1 (left) shows a schematic of a single receiver of the modules, while figure 1 (right) shows the EQE (external quantum efficiency) of the MJ solar cells and transmittance of the PMMA Fresnel lenses. As can be seen in figure 2 (top), the generator is formed by three modules connected in series and three branches in parallel. The modules are mounted on a two-axis tracker designed for point focus concentrators. The tracking mechanism of the system, settled in open loop to the irradiance and close loop with the position, allow a high accuracy to be reached - an error lower than 0.1 degrees. The array is connected to a high efficiency single-phase transformerless inverter with a high maximum DC/AC conversion of 96.6 % and a European weighted efficiency of 95 % (see figure 2 bottom). The main electrical characteristics of the whole HCPV system are shown in table 1. This system was installed at the CEAEMA in 2011, and the main electrical parameters and atmospheric variables were recorded daily every minute since that time. Further details regarding the characteristics, performance and experimental set-up used to carry out the evaluation of the system can be found in a previous work [38]. It is worth mentioning that the features of the modules [6], as well as the electrical configuration [44], represent the most wide-spread HCPV system nowadays. Thus, the results of this work can be considered representative of the current HCPV technology.

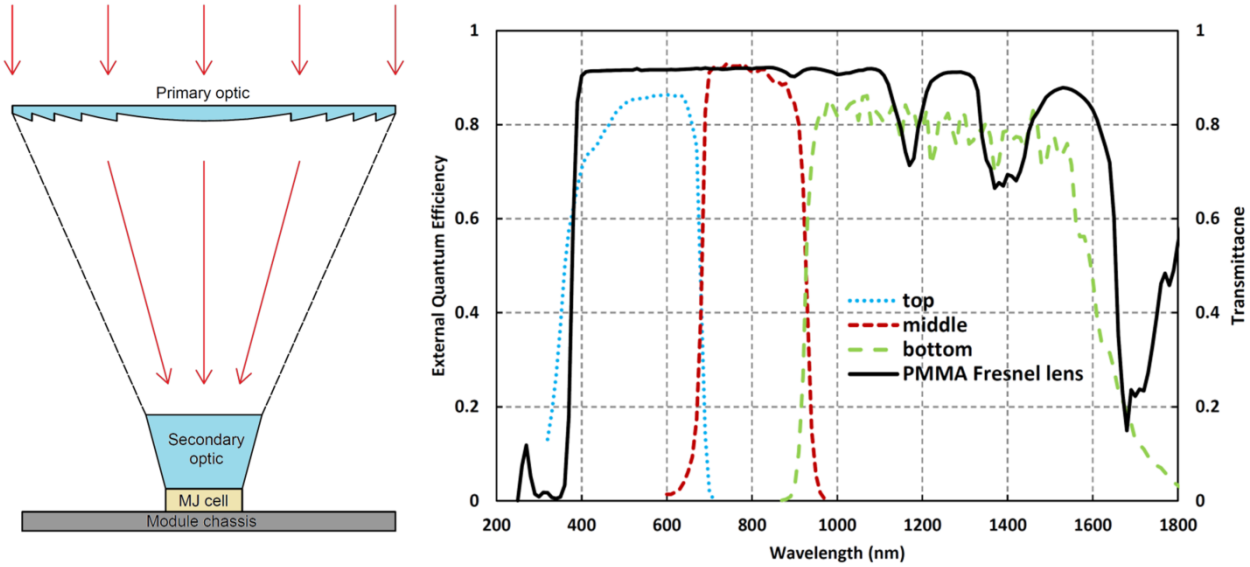

Figure 1. Left: Schematic diagram of an HCPV solar converter (generator) unit. Right: External quantum efficiency of the multi-junction solar cells and transmittance of the Fresnel lenses of the HCPV modules [38, 3].

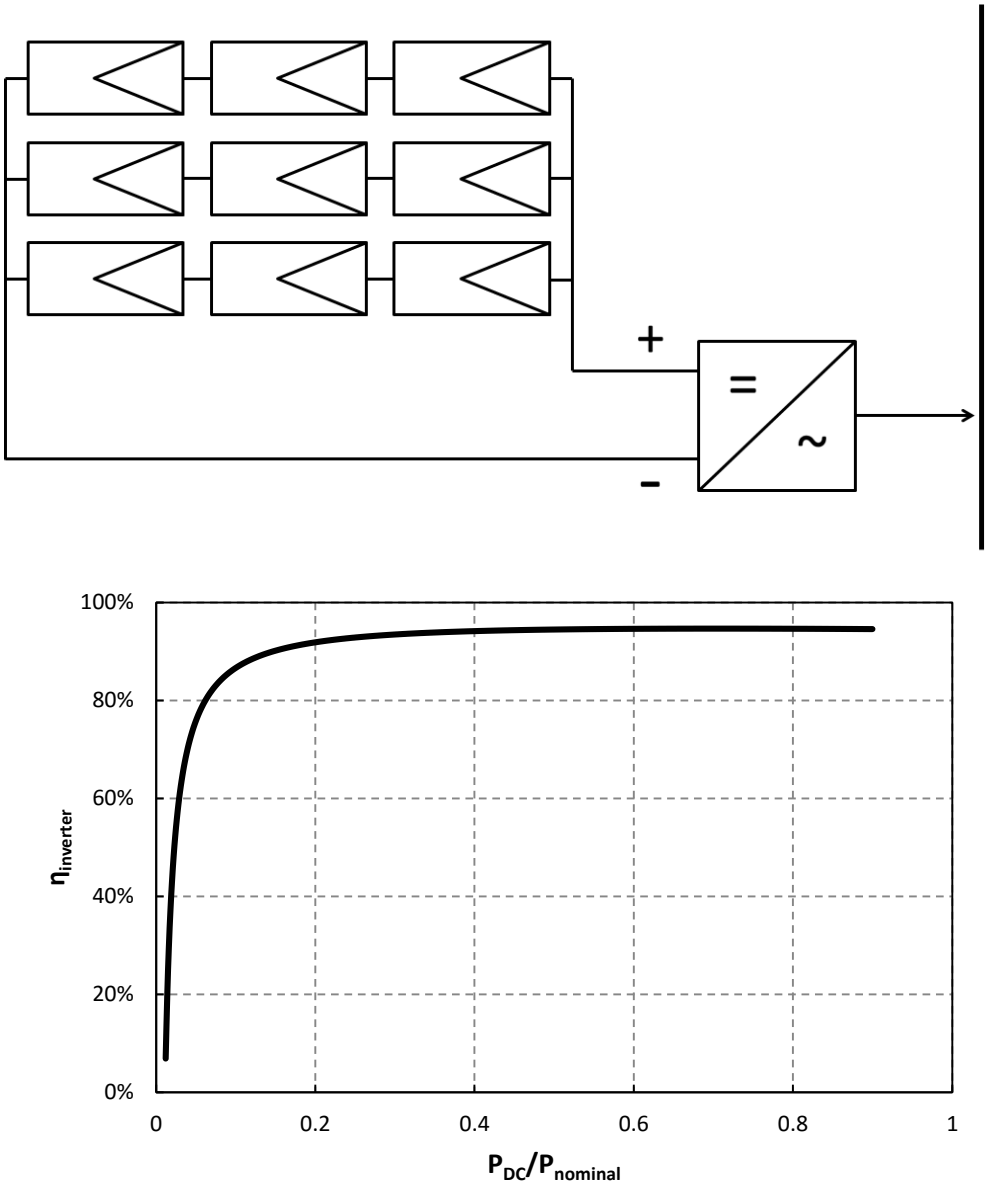

Figure 2. Top: Electrical configuration of the HCPV system. Bottom: Efficiency of the inverter as a function of the input DC power [38].

Parameter	**Value**
Short-circuit current (A)	7.2
Open-circuit voltage (V)	228
Current at the maximum power point (A)	6.9
Voltage at the maximum power point (V)	195
Maximum power (kW)	1.35

Table 1. Electrical characteristics of the HCPV system considered in this study under concentrator standard test conditions (CSTC) (1000 W/m^2, 25 ºC, AM1.5D) [45].

3. Model for estimating the energy yield

The energy yield of the HCPV system is estimated using the model previously introduced and experimentally validated by Fernandez et al. [38]. That model has been summarized and adapted to the goals and purpose of the present study. The modelling approaches and required input parameters for the model are outlined below in order to help the reader understand the discussion of the results shown in sections 4 and 5.

The power output of an HCPV module is mainly determined by the direct normal irradiance (DNI), cell temperature (T_c) and spectral distribution of the direct normal irradiance (S_b) as [46]:

$$P_{module} = f_{DNI} \cdot f_{T_c} \cdot f_{S_b} \quad (1)$$

The impact of DNI on the power can be estimated as a linear function of DNI as [24, 47]:

$$f_{DNI} = \frac{P^*}{DNI^*} \cdot DNI \quad (2)$$

where the superscript "*" refers to the values at reference conditions.

The influence of temperature can be evaluated with a linear temperature coefficient (δ) as [31, 30]:

$$f_{T_c} = 1 - \delta \cdot (T_C - T_c^*) \quad (3)$$

Among the different methods to estimate the cell temperature [33], it is appropriate to predict the value of T_c from atmospheric parameters as [29]:

$$T_c = T_{air} + R_{total} \cdot DNI_{heat} \quad (4)$$

where T_{air} the air temperature, R_{total} the thermal resistance of the module and DNI_{heat} the portion of DNI transformed into heat estimated as [48, 49]:

$$DNI_{heat} = DNI - \frac{P_{module}}{A_{module}} \quad (5)$$

The air mass (AM) and aerosol optical depth – usually evaluated at 550 nm – (AOD_{550}) has proved to be the relevant parameters to quantify the impact of the input solar spectrum on the long-term performance of HCPV devices [25, 34]. This influence can be evaluated with the following simple mathematical relationship [20, 50]:

$$f_{S_b} = (1 - \varepsilon \cdot (AM - AM_U))(1 - \varphi \cdot \left(AOD_{550} - AOD_{550,U}\right) \quad (6)$$

where ε and δ are the air mass and aerosol optical depth coefficients, and AM_U and $AOD_{550,U}$ are the umbral air mass and aerosol optical depth at which the power output begins to be influenced by AM and AOD_{550}.

The DC power (P_{DC}) delivered by the complete generator can be estimated considering its electrical configuration as:

$$P_{DC} = N_S N_P P_{module}(1 - L_{DC}) \quad (7)$$

where N_S and N_P are the number of modules in series and parallel respectively, and L_{DC} the additional DC losses of the HCPV generator such as shadowing, mismatch, soiling, wiring or misalignment.

The evolution of the instantaneous efficiency of the inverter ($\eta_{inverter}$) is mainly determined by the input DC power of the array and can be simulated as [51, 52]:

$$\eta_{inverter} = \frac{P_{AC}}{P_{DC}} = 1 - L_{inverter} \quad (8)$$

where P_{AC} the AC power of the system and $L_{inverter}$ the losses in the DC/AC conversion of the inverter given by [53]:

$$L_{inverter} = \frac{b_0 + b_1 p_{in} + b_2 p_{in}^2}{p_{in}} \quad (9)$$

where b_0, b_1 and b_2 are specific coefficients of the inverter that quantify the different DC/AC conversion power losses and p_{in} is the normalized inverted input power defined as:

$$p_{in} = \frac{P_{DC}}{P_{nominal}} \quad (10)$$

where $P_{nominal}$ is the nominal power of the inverter.

With the commented above, the AC power output of the whole HCPV system can be predicted as:

$$P_{AC} = P_{DC}(1 - L_{inverter})(1 - L_{AC}) \quad (11)$$

where L_{AC} is the additional losses produced in the AC part of the system such as the non-ideal performance of the inverter in the DC/AC conversion or downtime. Thus, the AC energy produced for a desired period of time T can be estimated as:

$$E_{AC} = \int_T P_{AC}\, dt \quad (12)$$

and the so-called final energy yield as:

$$Y_F = \frac{E_{AC}}{P_o} \quad (13)$$

where P_o is the peak power of the system.

The procedure above takes into account all the main parameters that affect the performance of an HCPV system by using simple mathematical relationships. Moreover, the model is entirely a function of atmospheric variables that can be obtained or calculated from atmospheric stations or databases in order to facilitate its application for long-term analysis at any desired site. Table 2 shows the values of the coefficients of the model for the system as previously presented by Fernández et al. [38]. It should be pointed out that some of the equations above have been reformulated when compared to those found in the reference [38], for instance those for f_{DNI}, f_{Tc} and f_{Sb}. The definition of these functions, in conjunction with the rest of equations of the model shown in this section, are the key to understanding the impact of the atmospheric parameters on the energy yield and LCOE of the system.

Coefficient	Value	Unit
R_{total}	0.059	$^oC/Wm^{-2}$
δ	0.12	%/^{o}C
ε	4.11	%
δ	32	%
AM_U	2.06	dimensionless
$AOD_{550,U}$	0.25	dimensionless
L_{DC}	4.41	%
b_0	0.010	dimensionless
b_1	0.023	dimensionless
b_2	0.023	dimensionless
L_{AC}	2.11	%

Table 2. Values of the coefficients obtained from outdoor monitored data for estimating the energy yield of the HCPV system considered.

4. Energy yield

The annual energy produced by the system described in section 2 has been estimated for the following 5 locations:

- Solar Village (Saudi Arabia): lat. N 24º54´25´´, long. E 46º23´49´´
- Alta Floresta (Brazil): lat. S 09º52´15´´, long. W 56º06´14´´
- Frenchman Flat (USA): lat. N 36º48´32´´, long. W 115º56´06´´
- Granada (Spain): lat. N 37´09´50'', long. W 03º36´18´´
- Beijing (China): lat. N 39º58´37´´, long. E 116º22´51´´

as previously considered by Fernández et al. [25, 34]. These sites represents worldwide regions over different continents with diverse climate conditions. Hence, it is possible to evaluate the

performance of the HCPV system in a wide range of working conditions. Table 3 gives the average values of the relevant weather parameters in order to show the atmospheric characteristics of each location.

The procedures to obtain the input parameters required by the model presented in section 3 are essentially the same as previously described and experimentally validated by the authors [3]. The input parameters used in this work are simulated, while they were obtained from an atmospheric station in the previous work [38] The DNI was simulated using the Simple Model of the Atmospheric Radiative Transfer of Sunshine (SMARTS) [54] as discussed by Fernández et al. [46, 25, 34]. The air mass was estimated from the sun´s position [55] while the daily time-series of aerosol optical depth at 550 nm was gathered from the Aerosol Robotic Network (AERONET) database [56]. Finally, the time-series of the air temperature was modelled from the maximum, minimum and average values obtained from NASA data sets [57] using the Erbs model [58, 59]. Once the inputs were available, the final energy yield of the system was obtained integrating the AC power every ten minutes for the whole year. A MATLAB^{TM} programming code was developed and used to carry out all the calculations. These results are shown in table 3. In addition, in order to have a sense of the accuracy of methodology used in this work, appendix I has also been included to compare the simulated and actual values of the annual energy output of the HCPV system under study. From this it is concluded that the resulting methodology is of good quality, with an error in the estimation of the annual energy yield of the HCPV system of less than 3%.

Location	**DNI (W/m^2)**	**T_{air} (^{o}C)**	**AM**	**AOD_{550}**	**Y_F (kWh/kW$_p$)**
Solar Village	694	28.8	3.0	0.35	2072
Alta Floresta	608	27.7	2.8	0.28	1829
Frenchman Flat	704	18.4	3.3	0.07	2302
Granada	623	19.1	3.3	0.15	1964
Beijing	390	15.7	3.4	0.82	1003

Table 3. Annual average values of the main atmospheric parameters (note that only values with DNI higher than 10 W/m^2 have been used to estimate the means of the variables) and simulated annual energy yield of the HCPV system for each site considered.

4.1. Impact of cell temperature and spectrum

As described above, table 3 shows the annual energy yield of the HCPV under study using the model described in section 3 and the obtained input parameters. As expected, the highest values of annual yield are produced for the locations with the highest DNI values. It was found that there exists a nearly linear relationship between the Final Energy Yield, Y_F, and the average DNI at the various locations. However, the increase of the annual yield with the annual average DNI is not perfectly linear (see figure 3). This can be explained due to the different impact of cell temperature and spectrum at each location produced by their diverse weather conditions, as shown in table 3. In order to clarify this issue, table 4 shows the annual average impact of direct normal irradiance, cell temperature and spectrum to better understand the impact of the weather variables listed in table 3 on the system for each location.

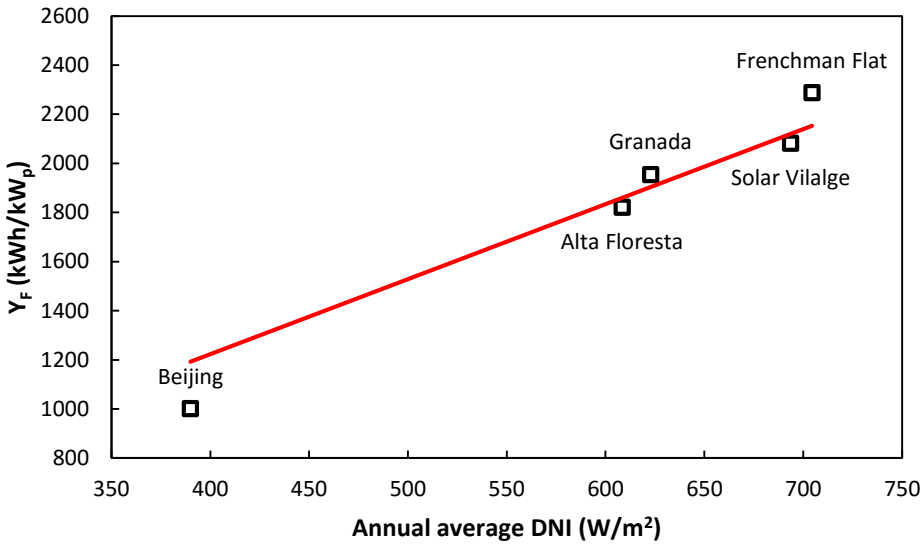

Figure 3. Final energy yield (Y_F) versus annual average direct normal irradiance (DNI) at each location.

Location	f_{DNI} (W)	f_{Tc}	f_{sb}
Solar Village	104	0.96	0.90
Alta Floresta	91	0.97	0.91
Frenchman Flat	106	0.97	0.93
Granada	93	0.98	0.93
Beijing	58	0.99	0.75

Table 4. Annual average impact of direct normal irradiance, cell temperature and spectrum for each site considered (note that only values with DNI higher than 10 W/m^2 have been used to estimate the means of the variables).

Figures 4 and 5 show the effect of cell temperature and spectrum, respectively, on the annual energy output at each site. The effect of cell temperature has been estimated as:

$$\Delta Y_{F,Tc} = \left(\frac{Y_F(DNI) - Y_F(DNI,T_c)}{Y_F(DNI)}\right) \cdot 100 \quad (14)$$

while the effect of spectrum has been estimate as:

$$\Delta Y_{F,Sb} = \left(\frac{Y_F(DNI) - Y_F(DNI,S_b)}{Y_F(DNI)}\right) \cdot 100 \quad (15)$$

As can be seen, the cell temperature AC energy losses range from 4.6 % to 1.8 %. Solar Village presents the highest losses due to the high DNI and T_{air} values, while Beijing presents the lowest losses due to the low DNI and T_{air} values. Regarding the spectral AC energy losses, they range from 5.0 % to 2.4 %, expect in Beijing. This location shows extreme spectral losses (21 %) due to its extremely high AOD_{550} values. Frenchman Flat presents the lowest AOD_{550} values and similar AM values compared with Granada (see table 3). However, the minimum spectral losses are produced at Granada. This can be explained, because this location has lower DNI values, and therefore the input DC power and efficiency of the inverter values are slightly lower. Therefore,

the contribution to the annual AC energy losses of AM and AOD_{550} are lower. This effect is explained below in more detail.

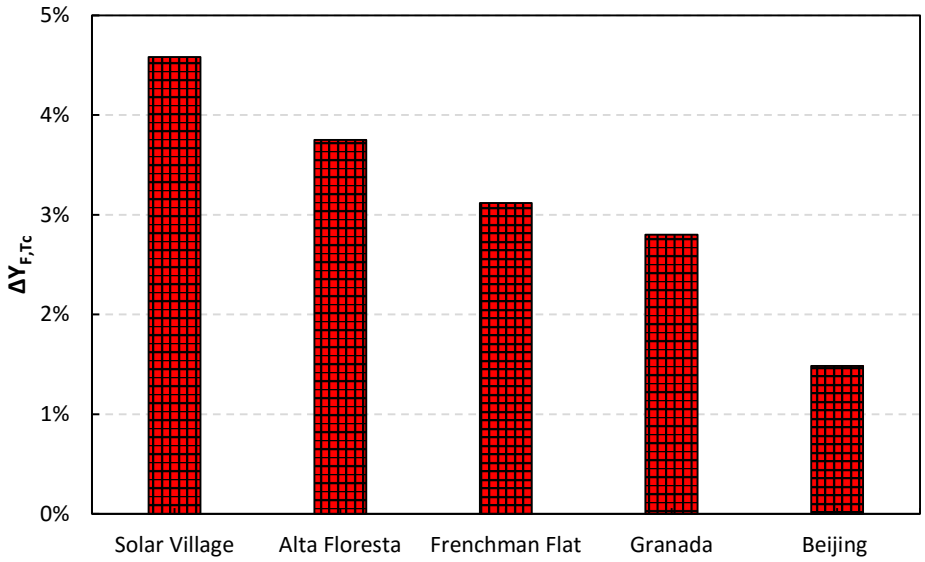

Figure 4. Annual energy cell temperature losses of the HCPV system for the five locations considered. See tables 3 and 4 to better understand the impact of cell temperature on the output of the system at each location.

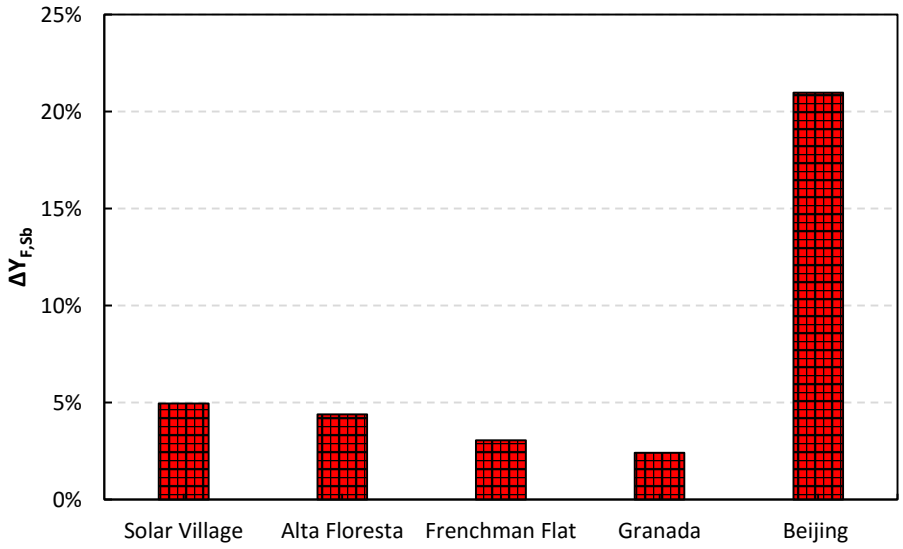

Figure 5. Annual energy spectral losses of the HCPV system for the five locations considered. See tables 3 and 4 to better understand the impact of spectrum on the output of the system at each location.

It can also be concluded that cell temperature and spectral AC energy losses are similar (expect in the case of Beijing); the cell temperature losses range from 4.6 % to 2.8 Solar Village % and the spectral losses range from 5.0 % to 2.4 %. This conclusion seems contrary to what is usually assumed, since the spectrum is considered to have a larger impact than cell temperature on the performance of HCPV devices [3]. In order to explain this finding, figures 6 to 9 show an example of the instantaneous impact on the output of cell temperature, spectrum, direct normal irradiance, as well as the efficiency of the inverter, for a summer and winter day at the Granada site. The same behaviour was found for the five locations analysed, with instantaneous cell

temperature losses between 0.9 and 1, and instantaneous spectral losses between 0 and 1. Based on these results, it may be stated that the spectral losses are higher than the thermal losses, as widely considered. However, the maximum thermal loses are produced at midday and during summer (see figure 6), when the contribution to the annual final yield is at maximum (see figure 8). In contrast, the maximum spectral losses are produced at sunrise and sunset and during winter (see figure 7) when the contribution to the annual energy yield is at a minimum (see figure 8). Moreover, the efficiency of the inverter is minimum at sunset and sunrise, and is maximum at midday (see figure 9). This means that the efficiency of the inverter is at a minimum when the higher spectral losses are produced, and is at a maximum when the higher cell temperature losses are produced. This explains why the effect of cell temperature and spectrum produce similar AC annual energy losses even though the instantaneous impact of the spectrum produces higher losses within the system. The comment above also highlights the importance of taking into account the coupling between the instantaneous effect of cell temperature and spectrum on the performance of the system, as well as the DC power of the generator and the efficiency of the inverter, to accurately estimate the temperature and spectral losses in the energy output of a real grid-connected HCPV system.

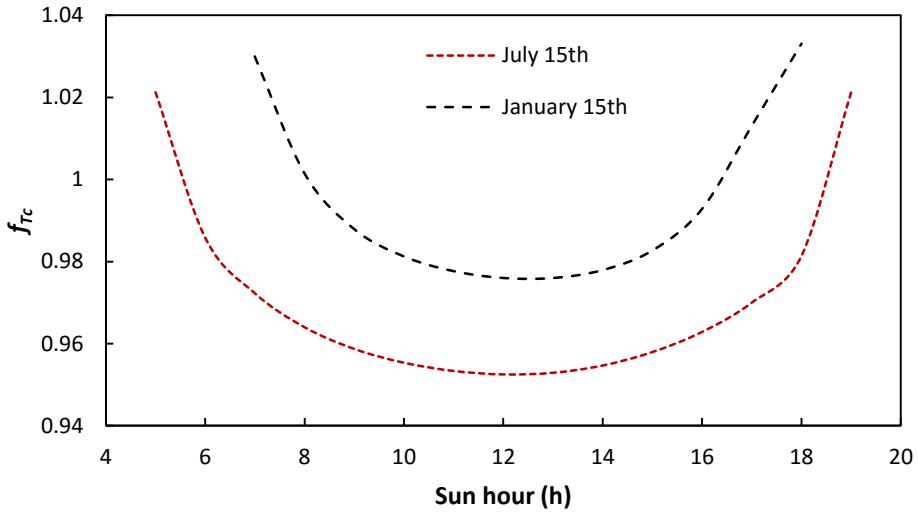

Figure 6. Instantaneous impact of cell temperature vs. sun hour, or solar time, for two example days at Granada.

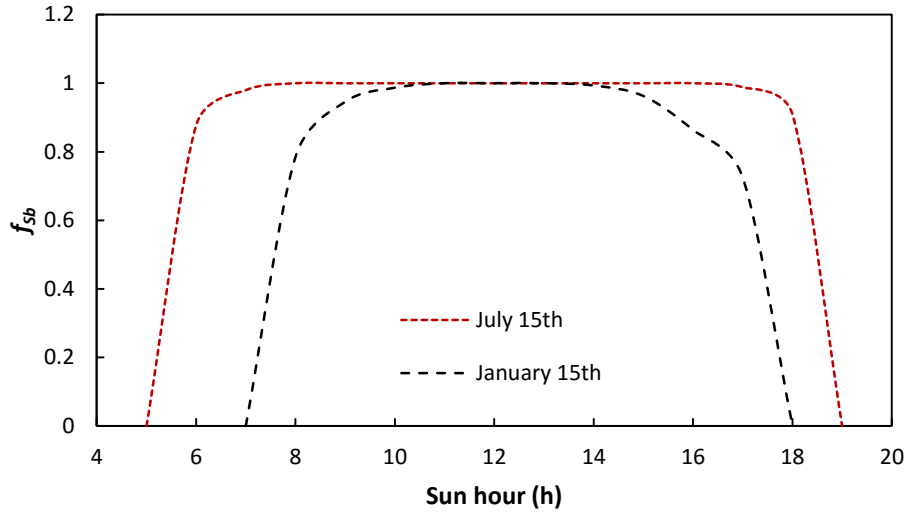

Figure 7. Instantaneous impact of spectrum vs. sun hour, or solar time, for two example days at Granada.

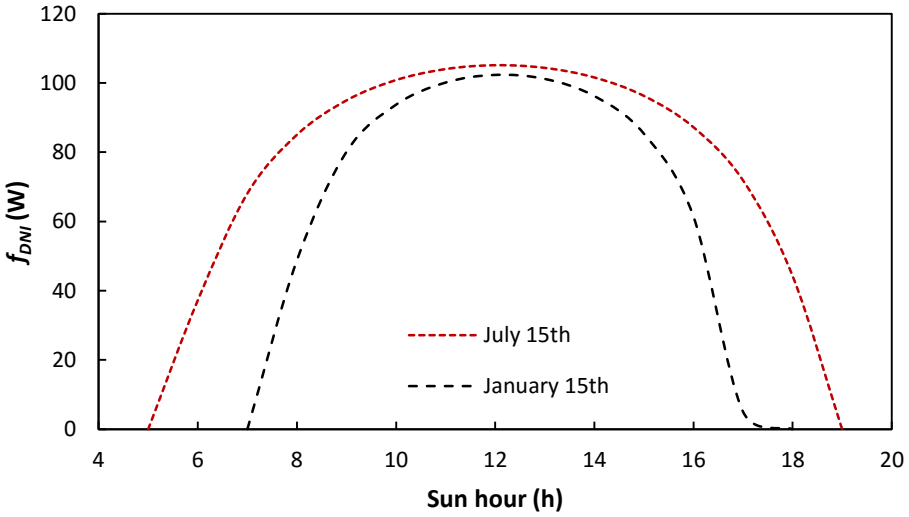

Figure 8. Instantaneous impact of direct normal irradiance vs. sun hour, or solar time, for two example days at Granada.

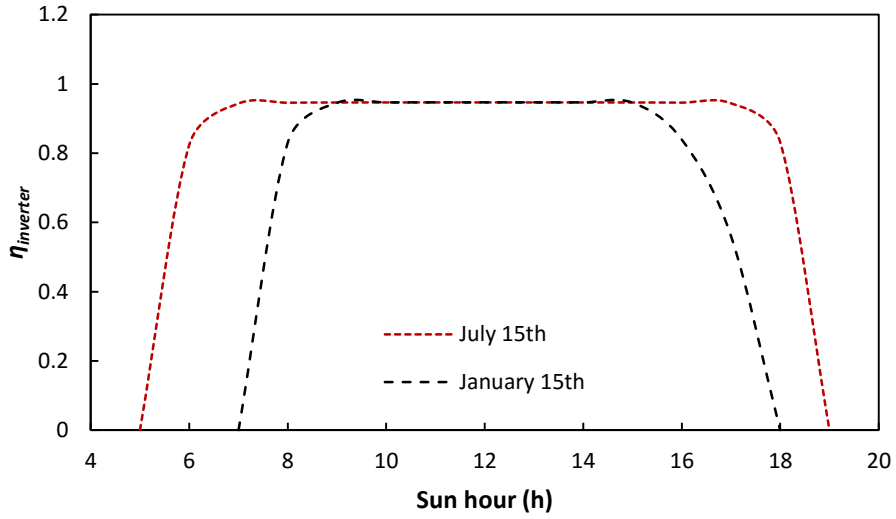

Figure 9. Instantaneous efficiency of the inverter vs. sun hour, or solar time, for two example days at Granada.

5. Cost of energy

In the previous section, the annual energy yield and the impact of cell temperature and solar spectrum on the annual energy output for the HCPV system have been analysed. Their values influence the cost of electricity of the HCPV system. So, in this section, the Levelised Cost of Electricity (LCOE) method has been applied to estimate the costs of energy of the system, and also to analyse the impact of cell temperature and input spectrum in these costs. Following the procedure introduced in previous works [60, 15], this parameter can be calculated as:

$$LCOE = \frac{LCC}{Y_F \frac{K_d (1 - K_d{}^N)}{1 - K_d}} \tag{16}$$

where the factor K_d is (1-r_d)/(1+d), where r_d is the annual degradation rate of the efficiency of the HCPV system, d is the nominal discount rate, N is the life cycle of the HCPV system and is LCC the normalized life cycle cost of the system. The annual final yield (Y_F) is assumed to remain constant over the life cycle of the system. The values for LCC can be estimated as:

$$LCC = HCPV_I + \mathrm{PW}[HCPV_{OM}(N)] - \mathrm{PW}[DEP(N_d)] \cdot T \tag{17}$$

This parameter mainly depends on the initial investment cost of the system ($HCPV_I$), the present worth of the operation and maintenance cost (PW[$HCPV_{OM}$(N)]) and the present worth of the tax depreciation (PW[DEP(N_d)]) (N_d is the period of time over which an investment is amortized for tax purposes and T is the income tax rate period.).

The initial investment cost may be financed through long-term debt or/and by means of equity capital. In the case where it is financed through a loan (debt) and the remainder by means of an issue of stocks (equity capital), it may be expressed as:

$$HCPV\,I = \left[HCPV_l \cdot \frac{i_l(1-T)}{1-(1+i_l(1-T))^{-N_l}} \cdot PVIF\,(N_l) \right] + \left[d_s \cdot HCPV_s \cdot PVIF\,(N) + HCPV_s \cdot q^N \right] \quad (18)$$

The first term in brackets of equation 18, related to the loan $HCPV_l$, is an amount of the initial investment cost that is borrowed at an annual loan interest (i_l) to be paid back in N_l years. This corresponds to the loan duration, where the impact of taxation on financing is taking into account (tax deduction applies to interest payments of loan). In this term, the present value interest factor is denoted as $PVIF(N_l)$, and is related to the nominal discount rate (d) by $PVIF(N_l) = q \cdot (1 - q^{N_l})/(1 - q)$, where $q = 1/(1+d)$. The second term of equation 18 corresponds to the issue of stocks $HCPV_s$, with an annual payback in the form of dividends (d_s) that must be paid in full at the end of the life cycle of the system. It is worth mentioning that equation 18 is only valid if the selected value of d is equal to the weighted average cost of capital (WACC) of the investment (the cost of the chosen financing). As shown above, d is involved in the calculation of the present value interest factors.

The present worth of the operation and maintenance cost of the life cycle system can be written as:

$$PW[HCPV_{OM}(N)] = \left(HCPV_{AOM}\,(1-T) \cdot \frac{K_{PV} \cdot (1 - K_{PV}{}^N)}{1 - K_{PV}} \right) \quad (19)$$

where $HCPV_{AOM}$ is the annual operation and maintenance cost, assumed constant over the life cycle of the system, K_{PV} is a factor that considers the annual escalation rate of the operation and maintenance cost of the system ($r_{O\&M}$), so $K_{PV} = (1+r_{O\&M})/(1+d)$.

Finally, the present worth of the tax depreciation that corresponds to the impact of taxation, is taken into account by assuming that the tax depreciation is deductible. In this case, the tax depreciation is assumed linear over the period time for which the HCPV system investment is amortized for tax purposes. Therefore, this term is expressed, bearing in mind that it represents a saving in the cash outflow, as:

$$PW[DEP(N_d)] = DEP_y \cdot PVIF(N_d) \quad (20)$$

where DEP_y is the annual tax depreciation of the HCPV system. The consideration of a linear tax depreciation implies that $DEP_y = HCPV_I/N_d$.

It should be highlighted that the weighted average cost of capital is the cost that must be paid by the owner or investor of the project for the use of capital sources in order to finance the investment. Organizations typically use the value of the organization's weighted average cost of

capital as nominal discount rate [61]. Following this strategy, in this work it is assumed that d is equal to WACC for the estimation of LCOE.

Table 5 lists the values of the parameters involved in the estimation of the LCOE using equation 16 for the five locations considered. The reasoning that leads to the selection of the parameters shown in this table is described below. It is important to mention that the procedure above has been formulated in terms of HCPV technology. However, the same methodology can be applied to estimate the LCOE of any type of solar energy or photovoltaics system.

Factors	**Location**					**Units**
	Solar Village	**Alta Floresta**	**Frenchman Flat**	**Granada**	**Beijing**	
Y_F	2072	1829	2302	1964	1003	kWh/kWp
$HCPV_I$	900 -2100					€/kWp
$HCPV_{AOM}$	2					%
r_d	0.5					%/year
$r_{O\&M}$	Equal to i					%/year
T	20	34	40	30	25	%
i	4.5	5.6	1.6	1.7	2.7	%
d	11.2	21.7	5.5	5.1	9.8	%
i_l	6.9	38.5	3.3	4.3	5.9	%
N_l	20					years
d_s	15.3	18.1	10	7.6	13.4	%
N	30					years

Table 5. Values of the factors assumed for the calculation of LCOE on HCPV systems for the five locations. It should be noted that the values presented here referring to costs, incentives and electricity yields are all normalized per unit of power (kWp).

The annual energy yield as a function of the atmospheric variables was presented in the previous section for the five sites considered. This is affected by the intrinsic degradation that the modules suffer throughout their lifetime. Therefore, the annual yield of the HCPV system is assumed to decrease every year. In this work, an annual degradation rate of 0.5 % has been considered [62, 63]. Finally, the time horizon of this cost analysis has been set to 30 years as previously considered by Talavera et al. [15].

The initial investment cost of the HCPV system is derived from the learning curve for HCPV technology. This curve describes the cost reduction as a function of the accumulated experience in the manufacturing and in the use of a particular technology. Previous studies [15, 16] analysed the cost of the initial investment during the period 2013-2020. As previously described, this initial investment cost may be financed by means of debt or/and equity capital. In this study, taking into account that commercial banks are generally accepting higher leverage in stable economies with secure property rights [64], it has been assumed that 70 % of this amount is borrowed as a loan, while the remaining investment amount (30 %) is contributed from equity capital, for the cases of Spain and the USA. For the remaining countries, the share of equity and debt for the project is assumed to be 50 %, as recommended by the CDM Executive Board [65]. Regarding the loan, this amount is borrowed at an annual interest that is specific for each

country. An average value for the period 2009-2013 has been considered for each specific location [66] and the loan term of 20 years has been considered for all of them. With regard to the equity capital, the annual payment of dividend is assumed to be specific for each country. As in the previous case, an average value for the period 1900-2000 has been considered for each location [67] and they will be payable completely at the end of the life of the PV system.

The data for the inflation rate has been obtained from the averages from historical data for each country in the period 2009-2013 [68, 69, 70]. The influence of the tax rate for the organization or taxpayer and its variations depending on each country's regulations have also been considered. In this analysis, the value of the income tax rate is assumed specific for each country [71, 72, 73]. The method used in the tax depreciation is based on a general method, using a maximum linear coefficient of 5 %, with a tax life for depreciation of 20 years for all countries [74, 75]. The nominal discount rate, which is considered equal to the weighted average capital of cost, is not constant and will vary depending on the capital resources chosen to finance the initial investment.

The normalised annual operation and maintenance costs of the HCPV system are considered as an annual fixed percentage (2 %) of the normalized initial investment cost of the HCPV system [76]. Additionally, these costs will also be influenced by an annual escalation rate, which was set equal to the value of the annual inflation rate the each country, so $r_{O\&M}$= i.

5.1. Impact of cell temperature and spectrum

Figure 10 shows the Levelised Cost of Electricity of the HCPV system under study using the procedure described above. In addition, table 6 shows some of the main economic parameters involved in the estimation of the LCOE for the five locations considered. In figure 10, the LCOE values at each location are plotted versus the initial investment cost since it has been demonstrated to have the largest impact, together with the annual energy yield, in its estimation. Other factors such as nominal discount rate, operation and maintenance cost and the life cycle of the HCPV system have been shown to have a moderate effect on the LCOE, while tax rate and power degradation rate have been shown to have an almost negligible influence [15, 77]. As can be seen, the locations with the higher annual energy yield tend to have the lower LCOE values. In particular, the lowest LCOE corresponds to Frechman Flat, with values ranging from 2.7 c€/kWh to 6.6 c€/kWh, while the highest LCOE corresponds to Beijing with values ranging from 10.6 c€/kWh to 24.7 c€/kWh. It should be also highlighted that a higher annual energy yield does not imply a lower value of LCOE, as can be clearly seen in Alta Floresta. This location has an annual energy yield (1829 kWh/KWp), higher than Beijing (1003 kWh/KWp) but its LCOE is slightly higher. This is mainly due to its high value of nominal discount rate (22.7 %) compared to the values of this parameter for the rest of the locations. Therefore, it is important to note that the sites with the highest final yield do not necessarily present the lowest values of LCOE, as clearly shown in figure 11. These results highlight the importance of considering the specific economic parameters that are involved in the estimation of the LCOE for the location under study.

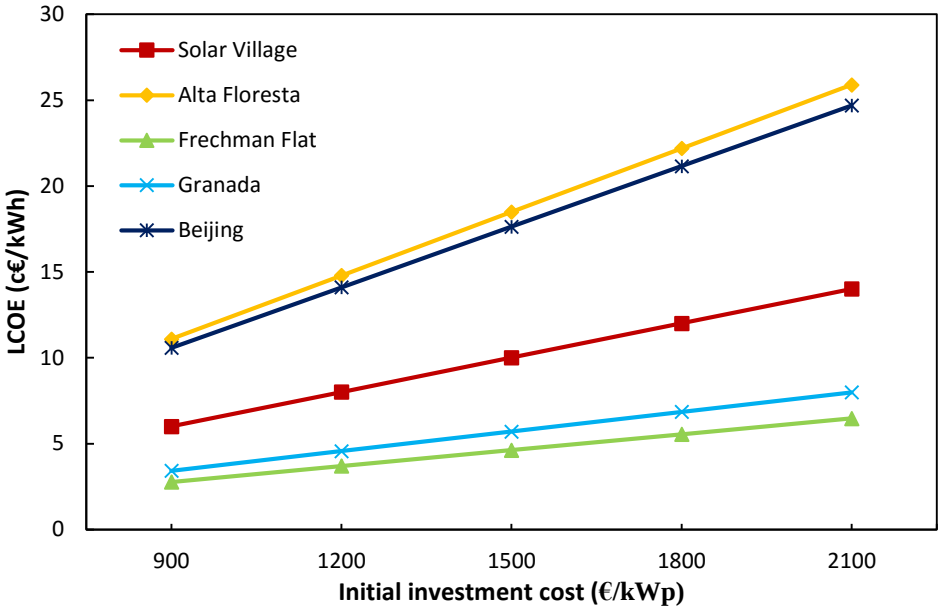

Figure 10. Levelised Cost of Electricity (LCOE) versus initial investment cost ($HCPV_I$) at each location.

Location	LCC (€/kWp)	PW[$HCPV_{OM}(N)$] (€/kWp)	PW[$DEP(N_d)$] (€/kWp)
Solar Village	2039	381	141
Alta Floresta	1816	154	138
Frenchman Flat	1751	381	430
Granada	1941	477	335
Beijing	1924	336	194

Table 6. Example of the main economic parameters involved in the estimation of the Levelised Cost of Electricity for the five locations under study. An initial investment cost of 1800 c€/kWp has been assumed.

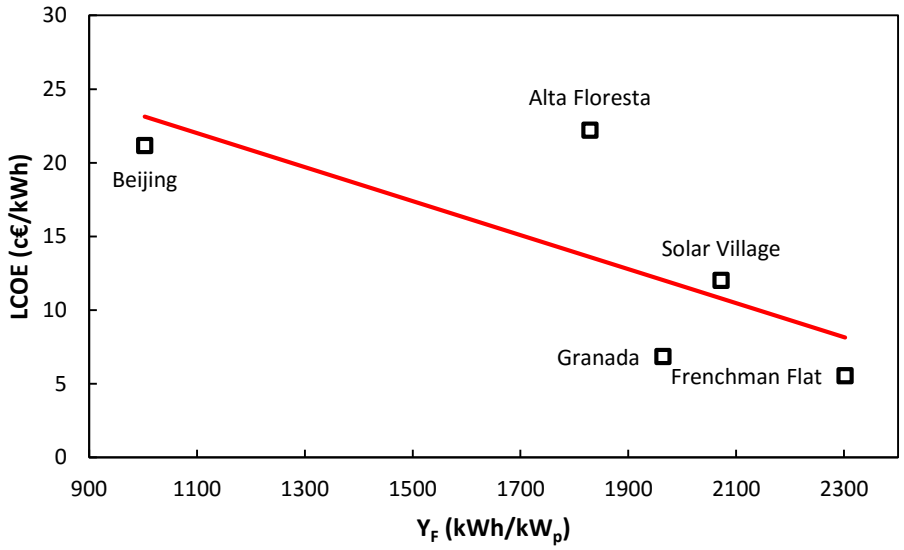

Figure 11. Levelised Cost of Electricity (LCOE) versus annual energy yield (Y_F) at each location. An initial investment cost of 1800 c€/kWp has been assumed.

Figures 12 and 13 show the effect of cell temperature and spectrum, respectively, on the Levelised Cost of Electricity at each site considering an initial investment cost of 1800 c€/kWp (conservative scenario [15]). The effect of cell temperature has been estimated as:

$$\Delta LCOE_{Tc} = LCOE(DNI, T_c) - LCOE(DNI) \quad (21)$$

while the effect of spectrum has been estimated as:

$$\Delta LCOE_{Sb} = LCOE(DNI, S_b) - LCOE(DNI) \quad (22)$$

As can be seen, the impact of cell temperature on the LCOE ranges from 0.17 c€/kWh (Frenchman Flat) to 0.80 c€/kWh (Alta Floresta). Regarding the impact of spectrum, the LCOE ranges range from 0.16 c€/kWh (Frenchman Flat and Granada) to 0.94 c€/kWh (Alta Floresta), without considering Beijing. The high AC energy spectral losses produced at this location lead to an extreme increase in its LCOE (4.37 c€/kWh). This demonstrates the importance of selecting locations with adequate weather characteristics to avoid significant increases in the cost of electricity produced by the spectral effects. It is worth mentioning that higher temperature and spectral AC energy losses do not necessarily produce a higher increase on the LCOE. This can be clearly observed comparing Solar Village and Alta Floresta (see figures 4 and 5). Solar Village has higher cell temperature and spectral losses than Alta Floresta, but the increase on the LCOE produced by these effects is lower. This can be explained by taking into account that the higher the LCOE, the higher the impact of temperature and spectral AC energy losses. Finally, the outcome of this work clearly indicates that the effect of cell temperature and spectrum on the energy yield needs to be considered in the analysis of the costs of the electrical generation of an HCPV system, since it could drive significant variations in the estimation of the LCOE.

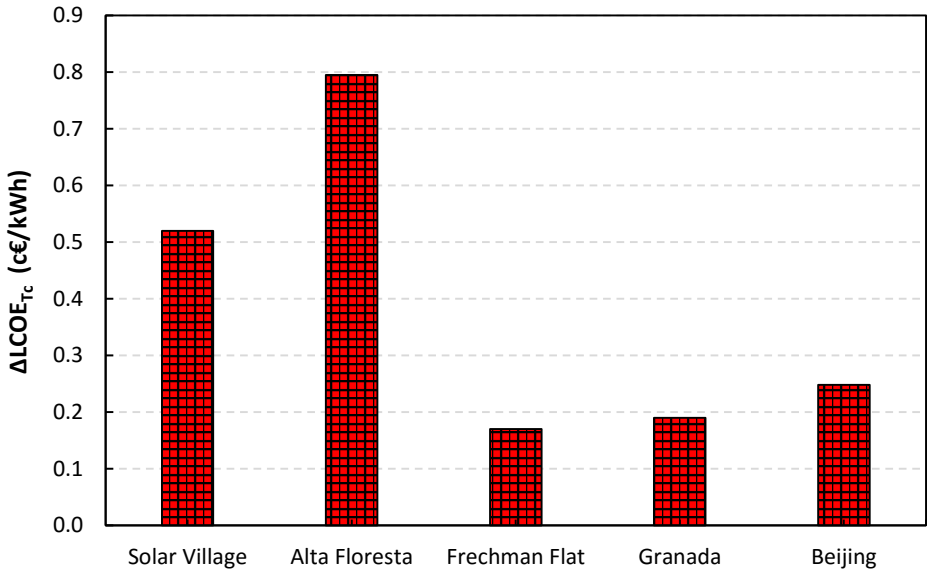

Figure 12. Impact of cell temperature on the Levelised Cost of Electricity (LOCE) of the HCPV system for the five locations considered. An initial investment cost of 1800 c€/kWp has been assumed.

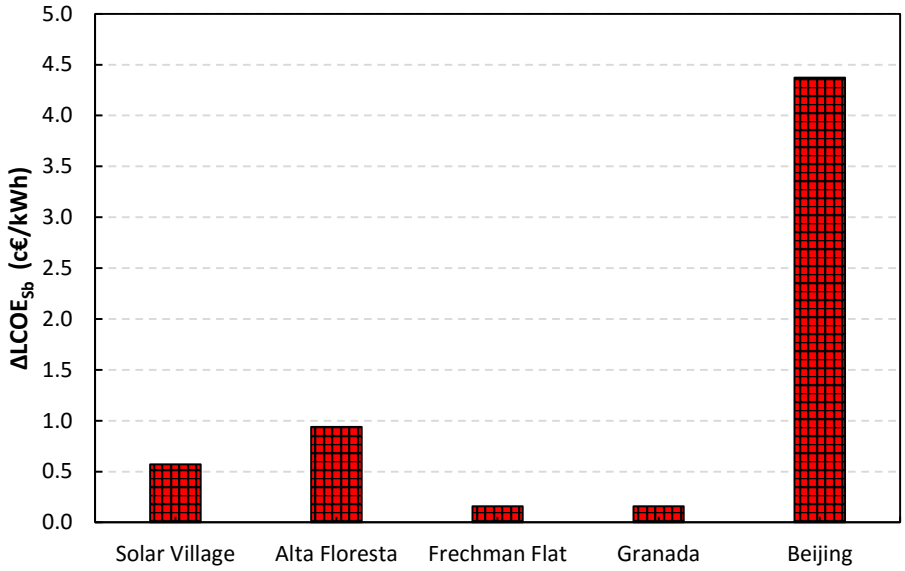

Figure 13. Impact of spectrum on the Levelised Cost of Electricity (LOCE) of the HCPV system for the five locations considered. An initial investment cost of 1800 c€/kWp has been assumed.

6. Conclusions

We have utilized the connections between the performance and economics of High Concentrator Photovoltaic (HCPV) technology to explore the cost of electricity of complete HCPV systems deployed in real-world settings. A typical state-of-the art system was studied experimentally at the Centre for Advanced Studies in Energy and Environment (CEAEMA) of the University of Jaen in Spain. Using experimental results for this system, its annual energy production has been estimated for deployment at five representative locations with diverse climatic conditions. The model used widely available data from meteorological and satellite databases.

The cell temperature and spectral AC energy losses were found to range, respectively, from 1.8 % to 4.6 % and from 5.0% to 2.4% (except in the case of a high polluted location). It can be concluded that the cell temperature and spectral AC energy losses are similar for the selected locations, contrary to what is often assumed. Analysis of the cell temperature and spectral AC energy losses led to the conclusion that it is the interrelationship between instantaneous cell temperature and input solar spectrum that affects the overall performance of the system.

Regarding the Levelised Cost of Electricity (LCOE), it was found, as expected, that locations with the higher annual energy yield tend to have the lower LCOE values. Sites with the highest final yield do not necessarily present the lowest values of LCOE, because of the importance of the specific economic parameters that are involved in the calculation of the LCOE, and the impact of cell temperature and spectrum. Values ranging from 2.7 c€/kWh to to 24.7 c€/kWh were obtained.

It may be concluded that at sunny locations with annual average DNI over 650 W/m^2, installations are expected to produce energy yields above 2000 kWh/kWp. Moreover, for a conservative scenario with an initial investment cost of under 1800 c€/kWp, the LCOE for state-

of-the-art HCPV solar power plants can be below 10 c€/kWh for many locations in the world. This highlights the ability of HCPV technology to produce large amounts of energy at competitive prices. Thus, this study supports the idea that HCPV can be a viable power source at locations with a favourable solar resource and economic scenarios. This work can therefore serve as a guide for further technical development of HCPV technologies, as well as for policy makers seeking to create economic conditions for their rapid deployment. Our analysis can be extended to include multiple modules and trackers in an HCPV array for a full solar power plant. This would allow for an estimation of the economics as a function of deployment scale.

Appendix I

As described, the mathematical model, as well as the procedures used to simulate the required input parameters, have been previously validated to estimate the electrical output of HCPV devices [38]. Despite this, a comparison between the simulated and experimental data for the HCPV system considered at the Granada AERONET site is presented in this appendix. It is important to mention that the system is located close to the Granada ground-based photometer of the AERONET data source. From among all the experimental years available, the data recoded during 2011 has been selected for the following two (main) reasons:

1. This year has the lowest (< 2.5 %) annual irradiation difference compared with the values obtained from statistical analysis or satellite measurements (PVGIS and SODA).
2. This year has not been used to fit the coefficients of the model shown in table 2.

This year was also selected in a prior work [38] to validate the mathematical model described in section 3 for the same two reasons as mentioned above. However, in that prior work, the input parameters to estimate the annual energy yield of the system were gathered from an atmospheric station, while in this case they are simulated. Despite this, the methodology used in this work shows high quality. There is difference lower than 3 % in the estimation of the annual energy yield and of around 2.5% in the estimation of the performance ratio (PR), as shown in table AI.1.

Parameter	Simulated	Experimental
Y_F (kWh/kW$_p$)	1964	1912
PR (%)	84	86

Table AI.1 Simulated and experimental values of the final energy yield (Y_F) and performance ratio (PR) of the HCPV system under study at the Granada AERONET site. The experimental data for the validation of the methodology used in in this work has previously been presented by Fernández et al. [38] (note that cloudy days have been removed in the estimation of the energy yield at each location by using the data provided by MODIS Daily Level-3 data source as previously considered [78, 79]).

Acknowledgements

This work is part of the project ENE2013-45242-R supported by the Spanish Economy Ministry and the European Regional Development Fund / Fondo Europeo de Desarrollo Regional (ERDF / FEDER). Eduardo F. Fernández is supported by the Spanish Ministry of Economy and Competitiveness through the Juan de la Cierva 2013 fellowship.

References

[1] A. Luque, G. Sala and I. Luque-Heredia, “Photovoltaic concentration at the onset of its commercial deployment,” *Progress in Photovoltaics: Research and Applications,* vol. 14, no. 5, pp. 413-428, 2006.

[2] H. Cotal, C. Fetzer, J. Boisvert, G. Kinsey, R. King, P. Hebert, H. Yoon and N. Karam, “III-V multijunction solar cells for concentrating photovoltaics,” *Energy and Environmental Science,* vol. 2, no. 2, pp. 174-192, 2009.

[3] E. F. Fernández, A. J. García-Loureiro and G. P. Smestad, “Multijunction concentrator solar cells: Analysis and fundamentals,” in *High Concentrator Photovoltaics: Fundamentals, Engineering and Power Plants, Pérez-Higueras, Pedro and Fernández, Eduardo F. (Eds.)*, Springer, 2015, pp. 9-37.

[4] W. T. Xie, Y. Dai, R. Wang and K. Sumathy, “Concentrated solar energy applications using Fresnel lenses: A review,” *Renewable and Sustainable Energy Reviews,* vol. 15, no. 6, pp. 2588-2606, 2011.

[5] M. Victoria, C. Dońminguez, I. Anťon and G. Sala, “Comparative analysis of different secondary optical elements for aspheric primary lenses,” *Optics Express,* vol. 17, no. 9, pp. 6487-6492, 2009.

[6] P. Rodrigo, L. Micheli and F. Almonacid, “The high-concentrator photovoltaic module,” in *High Concentrator Photovoltaics: Fundamentals, Engineering and Power Plants. Perez-Higueras, P.; Fernández, Eduardo F. (Eds)*, springer, 2015, pp. 115-151.

[7] A. Royne, C. Dey and D. Mills, “Cooling of photovoltaic cells under concentrated illumination: A critical review,” *Solar Energy Materials and Solar Cells,* vol. 86, no. 4, pp. 451-483, 2005.

[8] L. Micheli, N. Sarmah, X. Luo, K. Reddy and T. Mallick, “Oportunities and challenges in micro- and nano-technologies for concentrating photovoltaic cooling: A review,” *Renewable and Sustainable Energy Reviews,* vol. 20, pp. 595-610, 2013.

[9] L. Micheli, E. F. Fernández, F. Almonacid, T. K. Mallick and G. P. Smestad, “Performance, limits and economic perspectives for passive cooling of High Concentrator Photovoltaics,” *Solar Energy Materials and Solar Cells,* vol. Under review, 2016.

[10] E. Muñoz, P. Vidal, G. Nofuentes, L. Hontoria, P. Pérez-Higueras, J. Terrados, G. Almonacid and J. Aguilera, “CPV standardization: An overview,” *Renewable and Sustainable Energy Reviews,* vol. 14, no. 1, pp. 518-523, 2010.

[11] IEC_62108, “International Electrotechnical Commission. IEC 62108. Concentrator photovoltaic (CPV) modules and assemblies – Design qualification and type approval. 2007;Edition 1.0, Geneve.,” 2007.

[12] F. Gómez-Gil, X. Wang and A. Barnett, “Energy production of photovoltaic systems: Fixed, tracking, and concentrating,” *Renewable and Sustainable Energy Reviews,* vol. 16, no. 1, pp. 306-313, 2012.

[13] S. P. Philipps, A. W. Bett, K. Horowitz and S. Kurtz, “Current status of concetrator photovotailc (CPV) technology,” Fraunhofer ISE and NREL, 2015.

[14] F. Muñoz-Rodríguez, E. Muñoz-Cerón, F. Almonacid and E. F. Fernández, “Efficiencies and energy balance in high-concentrator photovoltaic devices,” in *High Concentrator Photovoltaics: Fundamentals, Engineering and Power Plants. Perez-Higueras, P.; Fernández, Eduardo F. (Eds)*, Springer, 2015, pp. 239-260.

[15] D. L. Talavera, P. Pérez-Higueras, J. Ruíz-Arias and E. F. Fernández, “Levelised cost of electricity in high concentrated photovoltaic grid connected systems: Spatial analysis of Spain,” *Applied Energy,* vol. 151, pp. 49-59, 2015.

[16] J. Haysom, O. Jafarieh, H. Anis, K. Hinzer and D. Wright, “Learning curve analysis of concentrated photovoltaic systems,” *Progress in Photovoltaics: Research and Applications,* vol. 23, no. 11, pp. 1678-1686, 2015.

[17] P. Perez-Higueras and E. F. Fernández, High Concentrator Photovoltaics: Fundamentals, Engineering and Power Plants, Springer, 2015.

[18] J. Aguilera, “Introduction,” in *High Concentrator Photovoltaics: Fundamentals, Engineering and Power Plants. Perez-Higueras, P.; Fernández, Eduardo F. (Eds)*, Springer, 2015, pp. 1-8.

[19] S. Kurtz, M. Muller, D. Jordan, K. Ghosal, B. Fisher, P. Verlinden, J. Hashimoto and D. Riley, “Key parameters in determining energy generated by CPV modules,” *Progress in Photovoltaics: Research and Applications,* vol. 23, no. 10, pp. 1250-1259, 2015.

[20] E. Fernández, P. Pérez-Higueras, A. Garcia Loureiro and P. Vidal, “Outdoor evaluation of concentrator photovoltaic systems modules from different manufacturers: First results and steps,” *Progress in Photovoltaics: Research and Applications,* vol. 21, no. 4, pp. 693-701, 2013.

[21] J. Leloux, E. Lorenzo, B. García-Domingo, J. Aguilera and C. A. Gueymard, “A bankable method of assessing the performance of a CPV plant,” *Applied Energy,* vol. 118, pp. 1-11, 2014.

[22] S. Philipps, G. Peharz, R. Hoheisel, T. Hornung, N. Al-Abbadi, F. Dimroth and A. Bett, “Energy harvesting efficiency of III–V triple-junction concentrator solar cells under realistic spectral conditions,” *Solar Energy Materials and Solar Cells,* vol. 94, no. 5, pp. 869-877, 2010.

[23] G. Kinsey and K. M. Edmondson, “Spectral response and energy output of concentrator multijunction solar cells,” *Progress in Photovoltaics: Reserch and Applications,* vol. 17, pp. 279 - 288, 2009.

[24] E. F. Fernández, G. Siefer, F. Almonacid, A. García-Loureiro and P. Pérez-Higueras, “A two subcell equivalent solar cell model for III–V triple junction solar cells under spectrum and temperature variations,” *Solar Energy,* vol. 92, pp. 221-229, 2013.

[25] E. F. Fernández, F. Almonacid, J. A. Ruiz-Arias and A. Soria-Moya, “Analysis of the spectral variations on the performance of high concentrator photovoltaic modules operating under different real

climate conditions," *Solar Energy Materials and Solar Cells,* vol. 127, pp. 179-187, 2014.

[26] R. Núñez, C. Domínguez, S. Askins, M. Victoria, R. Herrero, I. Antón and G. Sala, "Determination of spectral variations by means of component cells useful for CPV rating and design," *Progress in Photovoltaics: Research and Applications,* vol. DOI: 10.1002/pip.2715, in press.

[27] G. Siefer and A. Bett, "Analysis of temperature coefficients for III-V multijunction concentrator cells," *Progress in Photovoltaics: Research and Applications,* vol. 22, no. 5, pp. 515-524, 2014.

[28] E. F. Fernández, G. Siefer, M. Schachtner, A. García Loureiro and P. Pérez-Higueras, "Temperature coefficients of monolithic III-V triple-junction solar cells under different spectra and irradiance levels," *AIP Conference Proceedings,* vol. 1477, pp. 189-193, 2012.

[29] F. Almonacid, P. J. Pérez-Higueras, E. F. Fernández and P. Rodrigo, "Relation between the cell temperature of a HCPV module and atmospheric parameters," *Solar Energy Materials and Solar Cells,* vol. 105, pp. 322-327, 105.

[30] G. Peharz, J. Ferrer Rodríguez, G. Siefer and A. Bett, "Investigations on the temperature dependence of CPV modules equipped with triple-junction solar cells," *Progress in Photovoltaics: Research and Applications,* vol. 19, no. 1, pp. 54-60, 2011.

[31] E. Fernández, F. Almonacid, P. Rodrigo and P. Pérez-Higueras, "Calculation of the cell temperature of a high concentrator photovoltaic (HCPV) module: A study and comparison of different methods," *Solar Energy Materials and Solar Cells,* vol. 121, pp. 144-151, 2014.

[32] P. Rodrigo, E. F. Fernández, F. Almonacid and P. Pérez-Higueras, "Models for the electrical characterization of high concentration photovoltaic cells and modules: A review," *Renewable and Sustainable Energy Reviews,* vol. 26, pp. 752-760, 2013.

[33] P. Rodrigo, E. F. Fernández, F. Almonacid and P. J. Pérez-Higueras, "Review of methods for the calculation of cell temperature in high concentration photovoltaic modules for electrical characterization," *Renewable and Sustainable Energy Reviews,* vol. 38, pp. 478-488, 2014.

[34] E. F. Fernández, A. Soria-Moya, F. Almonacid and J. Aguilera, "Comparative assessment of the spectral impact on the energy yield of high concentrator and conventional photovoltaic technology," *Solar Energy Materials and Solar Cells,* vol. 147, pp. 185-197, 2016.

[35] N. Chan, H. Brindley and N. Ekins-Daukes, "Impact of individual atmospheric parameters on CPV system power, energy yield and cost of energy," *Progress in Photovoltaics: Research and Applications,* vol. 22, no. 10, p. 1080–1095, 2014.

[36] B. García-Domingo, J. Aguilera, J. de la Casa and M. Fuentes, "Modelling the influence of atmospheric conditions on the outdoor real performance of a CPV (Concentrated Photovoltaic) module," *Energy,* vol. 70, pp. 239-250, 2014.

[37] M. Renzi, L. Egidi and G. Comodi, "Performance analysis of two 3.5 kWp CPV systems under real

operating conditions," *Applied Energy,* vol. 160, pp. 687-696, 2015.

[38] E. F. Fernández, P. Pérez-Higueras, F. Almonacid, J. A. Ruiz-Arias, P. Rodrigo, J. I. Fernandez and I. Luque-Heredia, "Model for estimating the energy yield of a high concentrator photovoltaic system," *Energy,* vol. 87, pp. 77-85, 2015.

[39] P. Perez-Higueras and E. F. Fernandez, "High-concentrator photovoltaic power plants: Energy balance and case studies," in *High Concentrator Photovoltaics: Fundamentals, Engineering and Power Plants. Perez-Higueras, P.; Fernández, Eduardo F. (Eds)*, Springer, 2015, pp. 443-477.

[40] S. Tomosk, D. Wright, K. Hinzer and J. Haysom, "Analysis of present and future financial viability of high-concentrating photovoltaic projects," in *High Concentrator Photovoltaics: Fundamentals, Engineering and Power Plants. Perez-Higueras, P.; Fernández, Eduardo F. (Eds)*, 2015, pp. 377-400.

[41] D. Talavera and G. Nofuentes, "Economic evaluation of high-concentrator photovoltaic systems," in *High Concentrator Photovoltaics: Fundamentals, Engineering and Power Plants. Perez-Higueras, P.; Fernández, Eduardo F. (Eds)*, 2015, pp. 401-442.

[42] Fraunhofer Institute for Solar Energy Systems ISE, "Levelized cost of electricity renewable energy," 2013.

[43] W. Nishikawa, "LCOE concentrating photovoltaic for CPV," in *ICSC5 Conference*, 2008.

[44] E. Muñoz-Cerón, F. Muñoz-Rodríguez, J. De La Casa and P. Pérez-Higueras, "High-concentrator photovoltaic systems configuration and inverters," in *High Concentrator Photovoltaics: Fundamentals, Engineering and power plants. Perez-Higueras, P.; Fernández, Eduardo F. (Eds)*, Springer, 2015, pp. 209-237.

[45] IEC, "IEC 62670-1 ed1.0. Photovoltaic concentrators (CPV) - Performance testing - Part 1: Standard conditions," 2013.

[46] E. F. Fernández, F. Almonacid, A. Soria-Moya and J. Terrados, "Experimental analysis of the spectral factor for quantifying the spectral influence on concentrator photovoltaic systems under real operating conditions," *Energy,* vol. 90, p. 1878–1886, 2015.

[47] E. F. Fernández, P. Rodrigo, J. Fernández, F. Almonacid, P. Pérez-Higueras, A. García-Loureiro and G. Almonacid, "Analysis of high concentrator photovoltaic modules in outdoor conditions: Influence of direct normal irradiance, air temperature, and air mass," *Journal of Renewable and Sustainable Energy,* vol. 6, no. 1, 2014.

[48] E. F. Fernández and F. Almonacid, "A new procedure for estimating the cell temperature of a high concentrator photovoltaic grid connected system based on atmospheric parameters," *Energy Conversion and Management,* vol. 103, pp. 1031-1039, 2015.

[49] E. F. Fernández, P. Rodrigo, F. Almonacid and P. Pérez-Higueras, "A method for estimating cell temperature at the maximum power point of a HCPV module under actual operating conditions,"

Solar Energy Materials and Solar Cells, vol. 124, pp. 159-165, 2014.

[50] E. F. Fernández, F. Almonacid, T. Mallick and P. Pérez-Higueras, "Analytical modelling of high concentrator photovoltaic modules based on atmospheric parameters," *International Journal of Photoenergy,* vol. art. no. 872163, 2015.

[51] M. Jantsch, H. Schmidt and S. J., "Results on the concerted action on power conditioning and control," in *11th European photovoltaic Solar Energy Conference*, Montreux, 1992.

[52] K. Peippo and P. Lund, "Optimal sizing of solar array and inverter in grid-connected photovoltaic systems," *Solar Energy Materials and Solar Cells,* vol. 32, no. 1, pp. 95-114, 1994.

[53] J. Muñoz, F. Martínez-Moreno and E. Lorenzo, "On-site characterisation and energy efficiency of grid-connected PV inverters," *Progress in Photovoltaics: Research and Applications,* vol. 19, no. 2, pp. 192-201, 2011.

[54] C. Gueymard, "Parameterized transmittance model for direct beam and circumsolar spectral irradiance," *Solar Energy,* vol. 71, no. 5, pp. 325-346, 2001.

[55] F. Kasten and A. T. Young, "Revised optical air mass tables and approximation formula," *Applied Optics,* vol. 28, no. 22, pp. 4735-4738, 1989.

[56] "Aerosol Robotic Network (AERONET)," [Online]. Available: http://aeronet.gsfc.nasa.gov/. [Accessed 2015].

[57] "Surface meteorology and Solar Energy," [Online]. Available: https://eosweb.larc.nasa.gov/sse/. [Accessed 2015].

[58] F. Almonacid, P. Pérez-Higueras, P. Rodrigo and L. Hontoria, "Generation of ambient temperature hourly time series for some Spanish locations by artificial neural networks," *Renewable Energy,* vol. 51, pp. 285-291, 2013.

[59] D. Erbs, S. Klein and W. A. Beckman, "Estimation of degree-days and ambient temperature bin data from monthly-average temperatures," *Ashrae Journal,* pp. 60-65, 1983.

[60] D. L. Talavera, J. de la Casa, E. Muñoz-Cerón and G. Almonacid, "Grid parity and self-consumption with photovoltaic systems under the present regulatory framework in Spain: The case of the University of Jaén Campus," *Renewable and Sustainable Energy Reviews,* vol. 33, pp. 752-771, 2014.

[61] W. Short, D. J. Packey and T. Holt, "A manual for the economic evaluation of energy efficiency and renewable energy technologies," NREL/TP-462-5173, National Renewable Energy Laboratory, 1-120, 1995.

[62] K. Branker, M. J. Pathak and J. M. Pearce, "A review of solar photovoltaic level," *Renewable and Sustainable Energy Reviews,* vol. 15, pp. 4470-4482, 2011.

[63] D. C. Jordan and S. R. Kurtz, “Photovoltaic degradation rates - An Analytical Review,” *Progress in Photovoltaics: Research and Applications,* vol. 21, pp. 12-29, 2013.

[64] “UNEP/BNEF. Private financing of renewable energy: A guide for policymakers. Sustainable Energy Finance Initiative (UNEP), Bloomberg New Energy Finance (BNEF), Chatham House London, 2009,” [Online]. Available: http://fs-unep-centre.org/sites/default/files/media/financeguide20final.pdf. [Accessed 2015].

[65] “CDM Executive Board. Guidelines on the assessment of investment analysis. Bonn: UNFCCC Secretariat 2011,” [Online]. Available: https://cdm.unfccc.int/Reference/Guidclarif/reg/reg_guid03.pdf. [Accessed 2015].

[66] “World Bank. Lending interest rate 2015,” [Online]. Available: http://data. worldbank.org/indicator/FR.INR.LEND. [Accessed 2015].

[67] E. Dimson, P. Marsh and M. Staunton, “Equity Premiums around the World. Research Foundation Publications 2011: 32-35.,” [Online]. Available: http://www.cfapubs.org/doi/pdf/10.2470/rf.v2011.n4.5. [Accessed 2015].

[68] “European Central Bank. Inflaction in the Euro area 2014,” [Online]. Available: http://www.ecb.europa.eu/stats/prices/hicp/html/inflation.en.html. [Accessed 2015].

[69] “Trading Economics. Inflation Rate -Countries- List 2015,” [Online]. Available: http://www.tradingeconomics.com/country-list/inflation-rate. [Accessed 2015].

[70] “The World Bank. Inflation, consumer prices (annual %),” [Online]. Available: http://data.worldbank.org/indicator/FP.CPI.TOTL.ZG?page=1. [Accessed 2015].

[71] “Banco Santander. Portal Santander Trade 2015,” [Online]. Available: https://es.santandertrade.com/establecerse-extranjero/espana/fiscalidad. [Accessed 2015].

[72] “Ernst & Young Global Limited. Worldwide Corporate Tax Guide 2014 2014; EYG no. DL0917,” [Online]. Available: http://www.ey.com/Publication/vwLUAssets/Worldwide_corporate_tax_guide_2014/$FILE/Worldwide%20Corporate%20Tax%20Guide%202014.pdf. [Accessed 2015].

[73] “World Bank Group. Doing Business: Paying Taxes 2014,” [Online]. Available: http://www.doingbusiness.org/data/exploreeconomies/spain/#paying-taxes. [Accessed 2015].

[74] “Thonson Reuters. Consulta A.E.A.T. 128308, IS. Central fotovoltaica. Amortización. 2014.,” [Online]. Available: http://portaljuridico.lexnova.es/doctrinaadministrativa/JURIDICO/77405/consulta-aeat-128308-is-central-fotovoltaica-amortizacion. [Accessed 2015].

[75] “CREARA. PV Grid Parity Monitor Utility-scale, 2nd issue. September 2015. pp 15-17”.

[76] “Extance A, Márquez C. The Concentrated Photovoltaics Industry Report. CPV today 2010.”.

[77] C. Algora, D. Talavera, G. Nofuentes and I. Luque-Heredia, “Cost Analysis and Market Deployment,” in *Handbook of CPV Technology. Algora, C.; Rey-Stolle, I. (Eds)*, John Wiley & Sons, In press, pp. 733-782.

[78] “MODIS daily Level-3 data,” [Online]. Available: http://modis-atmos.gsfc.nasa.gov/MOD08_D3/. [Accessed 2015].

[79] E. Fernández and F. Almonacid, “Spectrally corrected direct normal irradiance based on artificial neural networks for high concentrator photovoltaic applications,” *Energy,* vol. 74, no. C, pp. 941-949, 2014.